Advances in Radiation Oncology (2022) 7, 100954

advances in radiation oncology

www.advancesradonc.org

Scientific Article

Single-fraction 34 Gy Lung Stereotactic Body Radiation Therapy Using Proton Transmission Beams: FLASH-dose Calculations and the Influence of Different Dose-rate Methods and Dose/Dose-rate Thresholds

Patricia van Marlen, MSc,* Wilko F.A.R. Verbakel, PhD, PDEng, Ben J. Slotman, MD, PhD, and Max Dahele, PhD, MBChB

Department of Radiation Oncology, Amsterdam UMC, Vrije Universiteit Amsterdam, Cancer Center Amsterdam, Amsterdam, the Netherlands

Received December 9, 2021; accepted March 21, 2022

Abstract

Purpose: Research suggests that in addition to the dose-rate, a dose threshold is also important for the reduction in normal tissue toxicity with similar tumor control after ultrahigh dose-rate radiation therapy (UHDR-RT). In this analysis we aimed to identify factors that might limit the ability to achieve this "FLASH"-effect in a scenario attractive for UHDR-RT (high fractional beam dose, small target, few organs-at-risk): single-fraction 34 Gy lung stereotactic body radiation therapy.

Methods and Materials: Clinical volumetric-modulated arc therapy (VMAT) plans, intensity modulated proton therapy (IMPT) plans and transmission beam (TB) plans were compared for 6 small and 1 large lung lesion. The TB-plan dose-rate was calculated using 4 methods and the FLASH-percentage (percentage of dose delivered at dose-rates ≥40/100 Gy/s and ≥4/8 Gy) was determined for various variables: a minimum spot time (minST) of 0.5/2 ms, maximum nozzle current (maxN) of 200/40 0nA, and 2 gantry current (GC) techniques (energy-layer based, spot-based [SB]).

Results: Based on absolute doses 5-beam TB and VMAT-plans are similar, but TB-plans have higher rib, skin, and ipsilateral lung dose than IMPT. Dose-rate calculation methods not considering scanning achieve FLASH-percentages between ∼30% to 80%, while methods considering scanning often achieve <30%. FLASH-percentages increase for lower minST/higher maxN and when using SB GC instead of energy-layer based GC, often approaching the percentage of dose exceeding the dose-threshold. For the small lesions average beam irradiation times (including scanning) varied between 0.06 to 0.31 seconds and total irradiation times between 0.28 to 1.57 seconds, for the large lesion beam times were between 0.16 to 1.47 seconds with total irradiation times of 1.09 to 5.89 seconds.

Conclusions: In a theoretically advantageous scenario for FLASH we found that TB-plan dosimetry was similar to that of VMAT, but inferior to that of IMPT, and that decreasing minST or using SB GC increase the estimated amount of FLASH. For the appropriate machine/delivery parameters high enough dose-rates can be achieved regardless of calculation method, meaning that a possible FLASH dose-threshold will likely be the primary limiting factor.

Sources of support: This work was sponsored by Varian.

Disclosures: WFAR Verbakel reports financial support was provided by Varian Medical Systems Inc. WFAR Verbakel reports a relationship with Varian Medical Systems Inc that includes: speaking and lecture fees and travel reimbursement. BJ Slotman reports a relationship with Varian Medical Systems Inc that includes: speaking and lecture fees and travel reimbursement. P van Marlen and WFAR Verbakel are members of the Varian FlashForward Consortium.

We do not have approval to share patient data or transfer it outside the institution. The code of the used scripts can be made available upon request.

*Corresponding author.; E-mail: p.vanmarlen@amsterdamumc.nl

https://doi.org/10.1016/j.adro.2022.100954

Introduction

In recent years, interest in ultrahigh dose-rate (UHDR; eg, ≥40 Gy/s) irradiation has increased greatly. Preclinical studies suggest that UHDR results in less normal tissue toxicity than conventional DR, while maintaining tumor control. This enhancement in therapeutic ratio by UHDR is called the FLASH-effect and has been observed in multiple in vitro and in vivo models.[1-5] Although the exact mechanisms of this effect are still unknown, thresholds for dose-rate and the dose seem to play an important role.[6-8] It is unclear whether a minimum dose threshold needs to be met or if the FLASH-effect increases with dose.[2] At this moment, dose thresholds up to 10 Gy have been mentioned[7,9] and if such values are accurate, there are not many types of plans that will achieve this dose in a single field/beam. Even though the high doses/fraction associated with stereotactic body radiation therapy (SBRT; typically 1-5 fractions of 6-30 Gy/fraction[10]) will not easily exceed the dose thresholds for a single beam, SBRT may still be one of the most suitable scenarios for FLASH-irradiation of deep-seated tumors.

SBRT plays a central role in the treatment of peripherally located, medically inoperable, early-stage non–small cell lung cancer (ES-NSCLC) and lung metastases.[11,12] Various SBRT fractionation schemes for ES-NSCLC, varying from 30 Gy in a single fraction to 60 Gy in 5 to 8 fractions, have demonstrated comparable results,[13,14] supporting the use of single-fraction schemes, with advantages of improved patient convenience and lower costs, for tumors in certain locations, away from critical organs.[15-18] Such high-dose single-fraction schemes are among those that are most likely to meet a potential FLASH dose threshold, making them interesting for UHDR treatment. In this analysis, we focus on single-fraction 34 Gy SBRT for peripherally located ES-NSCLC and small lung metastases as recently the Radiation Therapy Oncology Group (RTOG) 0915 trial showed no difference in toxicity and survival between 1 × 34 Gy and 4 × 12 Gy.[19,20] Furthermore, the lung is a suitable treatment site for the clinical translation of FLASH-radiation therapy, as lung fibrosis can serve as an in vivo indicator of radiation-induced damage and can be monitored and quantified.[21,22] Although lung toxicity was not an issue with single-fraction SBRT for a single lesion, treatment of multiple lung lesions, either primary lung cancers or metastases, is increasing and the risk of lung toxicity is a limiting factor in how many lesions can be treated.[23-25] A FLASH-effect in such situations could be beneficial.

Although most FLASH-experiments have used single, open electron,[1-5] and photon beams,[26] UHDRs can also be generated using proton beams,[7,27,28] with the advantage that they can treat larger and deep-seated tumors. In particular single, high energy transmission beams (TBs), where the Bragg-peak is placed outside the patient, seem to be the easiest and most practical option for UHDR proton treatment. No energy modulation is needed and they also have a steeper penumbra and increase robustness by eliminating range uncertainties. Proton UHDR TBs have demonstrated better plan quality than volumetric-modulated arc therapy (VMAT) for fractionated lung[29-31] and head and neck cancer[32] and have recently been selected for the first proton FLASH clinical trial,[33] but they have difficulty achieving similar healthy tissue sparing to intensity modulated proton therapy (IMPT), due to dose deposition behind the target.[32]

A recent publication, which also focused on FLASH for single-fraction 34 Gy lung SBRT, compared different dose-rate calculation methods and showed how they influence the estimated amount of FLASH-dose.[34] It has become clear that not only the dose-rate, but other factors such as the dose delivered in a certain period of time should also be taken into account. Additionally, it is useful to translate the FLASH-dose into a clinically relevant outcome, which also makes comparison with other treatment plans possible. In this study we have therefore focused on the following aspects of UHDR-delivery of single-fraction lung SBRT: (1) plan quality comparison of UHDR proton TB with VMAT and IMPT; (2) analysis of the amount of FLASH using not only multiple dose-rate calculation methods, but also various (more and less-favorable) dose and dose-rate thresholds and (machine) parameter settings; and (3) quantification of the FLASH-effect on TB-plans by calculating a FLASH-modified dose (FMD) based on dose and dose-rates.

Methods and Materials

Treatment planning and quality comparison

This work was conducted as part of an Institutional Review Board approved retrospective treatment planning protocol. Six anonymized clinical computed tomography (CT) scans with a single, small, peripherally located lung tumor, either ES-NSCLC (n = 4) or a lung metastasis (n = 2), were randomly selected from the group of patients treated with 1 × 34 Gy. The internal planning volume (ITV), defined using a 10-phase free-breathing 4-dimensional CT scan, was 1.39 to 8.58 cm^3 and the planning target volume (PTV; ITV + 5 mm margin), was 7.70 to 19.02 cm^3. All tumors had been clinically treated with a

single fraction of 34 Gy using a dual-arc photon VMAT treatment plan (RapidArc, Varian Medical Systems, Palo Alto, CA). For comparative purposes, a seventh, substantially larger lung tumor (ITV 54.54 cm^3, PTV 107.78 cm^3), was included.

For each of the 7 patients 4 coplanar proton plans were made (research version Eclipse treatment planning system, Varian Medical Systems): 3 TB-plans using either a 3-, 5-, or 10-beam setup, and one 3-beam IMPT-plan. The beam energy of the TBs was 250MeV, which was sufficient to place the Bragg-peak outside the patient and irradiate only with the proximal beam section. The IMPT-plans were robustly optimized, taking 5 mm isocenter shifts and 3% range uncertainties into account.

All proton plans, both TB and IMPT, were made with the support of the Python Eclipse Scripting Application Programming Interface (PyESAPI, Varian Medical Systems) and used multifield optimization to optimize spot weights (Eclipse-PT, Varian Medical Systems). Fixed minimum (ITV, PTV) and maximum (PTV, ring, spinal cord, trachea, aorta, esophagus, skin, rib, contralateral lung, heart) dose volume objectives were used, while mean dose objectives (skin, rib, lungs minus ITV, contra- and ipsilateral lung, heart) were variable. Three rounds of optimization were performed, iteratively adjusting the mean dose objectives to 90% of their respective mean dose value. After the last optimization, spots with <100 monitor units (MU) were removed. All proton plans prioritized avoidance of the spinal cord, contralateral lung, and heart, and were normalized such that 95% of the PTV received 100% of the prescription dose (V100% = 95%), ITV V95% ≥115% and PTV maximum dose up to 140%. The plan quality was compared with that of the clinical VMAT plan and was also evaluated using dose volume histograms (DVHs) and PTV, ITV, and OAR dose statistics, the latter of which were benchmarked against the dose constraints from the RTOG 0915 trial.[19,20] Although TB-delivery is so quick that it could be done during a brief breathhold, possibly enabling planning on the GTV instead of ITV, we used the ITV to allow for a better comparison with VMAT and IMPT.

Dose-rate analyses

TB-plan data such as 3-dimensional (3D) spot doses, structures and spot parameters were obtained using PyESAPI and loaded into Matlab (version R2018b, MathWorks, Natick, MA) to perform dose-rate calculations. In most UHDR-research using single, open beams, the dose-rate is described as the total (beam) dose divided by the entire irradiation time. For proton pencil-beam scanning (PBS) delivery, the definition of dose-rate is not as straightforward, as multiple spots (and beams) deliver dose to a certain voxel sequentially. This has led to a variety of dose-rate calculation methods,[35] each making their own assumptions. In this article we consider the following 4 methods: (1) UHDR-contribution (UHDRc)[29,32]; (2) dose-averaged dose-rate (DADR)[36]; (3) PBS dose-rate (PBS-DR)[35]; and (4) average dose-rate (ADR).

The first 2 methods, UHDRc and DADR, use the voxel-specific dose-rate distribution resulting from the different spot dose-rates of each spot. The spot dose-rates are defined as the voxel spot dose divided by the spot irradiation time. We assume spot-by-spot scanning, which means that the beam only irradiates when located at the spot-center and is turned off during scanning. Because doses are only delivered during the so-called spot beam-on times, we chose to use these times in the spot dose-rate calculations. After obtaining the voxel-specific dose-rate distribution, the UHDRc and DADR could be calculated. The UHDRc is defined as the percentage of local dose delivered at UHDRs:

$$UHDR_c(x,y,z) = \left(\sum_{i:\ dr_i(x,y,z) \geq T_{DR}} \frac{D_i(x,y,z)}{D_{tot}(x,y,z)} \right) \cdot 100\%$$

with dr_i the spot dose-rate of spot i at voxel (x,y,z), D_i the spot dose of spot i at voxel (x,y,z), D_{tot} the total beam dose at voxel (x,y,z), and T_{DR} the UHDR-threshold. This method has been described in 2D earlier,[29,32] but we use it in 3D. The DADR gives the dose-rate averaged over all spots, weighted by the dose share of each spot to a voxel:

$$DADR(x,y,z) = \sum_i \frac{dr_i(x,y,z) \cdot D_i(x,y,z)}{D_{tot}(x,y,z)}$$

The third method, the PBS-DR, takes a different approach and includes scanning time in its calculations, thereby acknowledging the temporal element of PSB delivery. It points out that most of the dose accumulation at a voxel occurs during a short time because only a limited number of spots delivers a significant dose to a voxel. The PBS-DR in a beam voxel is therefore calculated by only considering a certain substantial part of the voxel dose and the time it takes to deliver that dose:

$$PBS-DR(x,y,z) = \frac{D_{tot}(x,y,z) - 2 \cdot T_{D,PBS}(x,y,z)}{t_1(x,y,z) - t_0(x,y,z)}$$

This equation formulates how the effective irradiation time starts at t_0, when the voxel dose surpasses a certain dose threshold $T_{D,PBS}$, and ends at t_1, when the total voxel dose minus the dose threshold is reached. We chose a fixed $T_{D,PBS}$ of 1cGy, similar to the threshold previously used in the literature.[35]

The fourth method, the ADR, gives the total local dose divided by the total irradiation time and therefore also includes the time to deliver spots far away from the location. This is the dose-rate mentioned by most single, open beam UHDR-research.

Because multiple dose-rate thresholds have been mentioned,[7] we have chosen to do our dose-rate calculations for an UHDR-threshold T_{DR} of both 40 Gy/s and 100 Gy/s, which are usually the lowest and highest dose-rate threshold mentioned in the literature.

Energy-layer based gantry current vs spot-based gantry current

The gantry-current (GC) is an important determinant of the irradiation time and can be varied using 2 different techniques. Usually the GC is constant for the entire energy-layer and scaled to deliver the lowest spot MU in the shortest possible spot time (energy-layer based [EB] GC). Another possibility, not yet clinically available, is to vary the GC per spot (spot-based [SB] GC), meaning that all spots are irradiated for the minimum spot time (if feasible, otherwise delivered at highest achievable current). This can greatly decrease irradiation time and we were interested in how these 2 GC techniques affected the dose-rate and FLASH-modified dose. A minimum spot time of 2 ms is currently clinically achievable,[37] but was assumed to get as low as 0.5 ms, which is not yet clinically available, but is technically feasible on certain machines.[38,39]

FLASH-modified dose

The biological mechanism responsible for the FLASH-effect remains unclear, making it difficult to calculate a definitive FLASH-effect from the treatment plan. Although some theories claim that avoidance of radiating circulating immune cells are of importance in mediating the normal tissue protective effect,[40] oxygen depletion is more frequently proposed as an explanation.[41-44] Assuming that oxygen depletion is an important contributor to the FLASH-effect, a dose and dose-rate threshold will be relevant,[45] which is confirmed by most preclinical studies. We therefore based our estimated FMD not only on dose-rate threshold T_{DR}, but also on a dose threshold. In many articles a minimum of 10 Gy is believed necessary for FLASH,[7,9] but in recent studies the FLASH-effect was observed for doses as low as 7 Gy[5] and 4 Gy.[46] For that reason we analyzed the FMD for a dose threshold T_D of 4 Gy and 8 Gy. Both the dose and dose-rate analyses were executed for each beam separately because the time between beam irradiations is far higher than the time necessary to reoxygenate the tissue (reoxygenation through diffusion is in the order of 10^{-3}s to 10^{-2}s,[44] while time between beams is >30 s) and we assumed the environment had been restored to its initial state before a subsequent beam irradiation.

For all dose-rate methods the amount of voxel beam dose delivered at dose-rates higher than T_{DR} was determined and when this dose exceeded the dose threshold T_D, it was considered FLASH-dose. The FLASH-dose was adjusted by dividing the physical dose by a FLASH-factor. The exact value of the FLASH-factor is unknown, but it has been estimated between 1.1 to 1.8,[7] suggesting the FLASH-effect would equal a dose reduction of ~10% to 45%. FLASH-modification was only applied to tissue outside the ITV and we considered 3 FMD scenarios for FLASH-factors of 1.4 and 1.8, a clinically achievable scenario (minST = 2 ms, maxN = 200 nA, EB GC) with FLASH-thresholds of 4 Gy and 40 Gy/s and 2 best case scenarios (minST = 0.5 ms, maxN = 400 nA, SB GC): the first with FLASH-thresholds of 4 Gy and 40 Gy/s and the second with FLASH-thresholds of 8 Gy and 100 Gy/s.

Results

Plan comparison

VMAT, IMPT, and TB-plan dose statistics and the RTOG 0915 constraints are given in Table 1. The 5-beam TB-plans are illustrated in Fig. E1 and Fig. E2 shows the VMAT, IMPT, and 5-beam TB-plan, and DVH, for a single lesion. RTOG 0915 constraints were met for all OARs in all plans. Note that the RTOG requirements are defined for lungs-GTV instead of lungs-ITV; however, even evaluating the entire lungs will not result in the limits set by RTOG 0915 being exceeded. In contrast with Bragg-peak proton beams, TBs have a reasonably constant dose depth profile, with the entry dose comparable to the dose in the target. This led to high skin and rib doses for the 3-beam TB-plans, and 5-beam and 10-beam plans achieved better sparing. Because the plan quality of 5- and 10-beam plans was comparable and a possible dose threshold for FLASH is more easily reached with fewer beams, we focused the remaining FLASH analyses only on the 5-beam TB-plans. TB-plans using 3 beams were not considered for the analyses as the corresponding plan quality was insufficient. Compared with VMAT and IMPT, TB-plans achieved better/similar sparing of spinal cord, esophagus, trachea, and heart. However, IMPT was better for ribs (mean dose + 0.8 Gy), skin (mean dose + 0.5 Gy), and lungs, with in particular larger lung volumes receiving ≤10 Gy (V5 Gy/V10 Gy + 30%/+ 46%).

Dose-rate analyses

Table 2 gives the FLASH-percentages for all dose-rate calculation methods and multiple FLASH-requirements and machine parameters. The FLASH-percentage is the percentage of dose delivered at dose-rates higher than T_{DR} and exceeding T_D. The chosen values for the minimum spot time (minST)/maximum nozzle current

Table 1 dose statistics of VMAT, IMPT and TB-plans for 3-, 5- and 10-beams (3b, 5b, 10b). Maximum and mean doses are given in Gy, volume receiving *x* Gy (V*x*Gy) in cm^3. Column 'RTOG 0915' lists the requirements given by the RTOG 0915 trial. Columns '1-6' give the averages for patients 1-6 (small lung lesions), columns '7' the dose statistics of patient 7 (larger tumor). Empty cells denote zeros.

Structure	*Metric*	*RTOG 0915*	*VMAT*		*IMPT*		*TB 3b*		*TB 5b*		*TB 10b*		*TB 5b-VMAT*	*TB 5b-IMPT*
			1-6	*7*	*1-6*	*7*	*1-6*	*7*	*1-6*	*7*	*1-6*	*7*	*1-6*	*1-6*
Spinal cord	max	14Gy	4.1	7.5	0.3	6.3	3.4	10.7	2.0	8.3	2.2	7.6	**-2.1***	1.7
	V10Gy	<0.35cm^3												
	V7Gy	<1.2cm^3						1.0		0.1				
Esophagus	mean		1.6	6.0	0.1	1.6		1.7		2.9		3.3	**-1.6****	-0.1
	max	15.4Gy	4.0	12.0	1.0	9.7		8.8	0.4	6.8	0.9	6.0	**-3.6****	-0.6
	V11.9Gy	<5cm^3												
	V8Gy			2.9		0.1		0.1						
Heart	mean		0.9	0.2	0.5		0.5		0.5		0.5		**-0.4***	-0.1
	max	22Gy	7.0	0.4	4.9		6.9		6.5		6.6		-0.4	1.6
	V16Gy	<15cm^3												
Trachea	mean		0.6	6.4	0.1	2.2		4.1		4.3		3.4	-0.6	-0.1
	max	20.2Gy	4.6	16.3	2.2	9.8	1.2	14.1	0.4	9.5	0.5	9.5	**-4.2***	-1.8
	V10.5Gy	<4cm^3		3.3				1.8						
	V8Gy			6.5		0.1		4.7		1.5		0.8		
Ribs	mean		2.2	5.8	0.8	2.9	1.6	5.0	1.5	5.1	1.5	4.9	**-0.6****	**0.8****
	max	30Gy	21.0	38.1	22.2	36.5	25.1	37.3	23.1	36.4	22.6	36.7	2.1	0.9
	V22Gy	<1cm^3	1.4	58.7	1.0	42.9	1.8	57.0	1.2	51.5	1.1	54.7	-0.1	0.2
	V16Gy		6.3	127.1	3.0	71.8	12.6	83.4	5.4	87.4	4.4	83.8	-0.9	2.4
	V12Gy		22.3	176.8	9.1	97.0	50.9	207.7	18.5	120.2	13.8	116.0	-3.8	9.4
Skin	mean		1.2	4.0	0.4	1.1	1.0	4.1	0.9	3.8	0.9	3.9	**-0.3****	**0.5****
	max	26Gy	9.4	16.4	10.9	12.9	18.0	18.7	14.1	15.1	12.7	13.8	**4.7****	3.2
	V23Gy	<10cm^3	0.1										-0.1	
	V16Gy						1.3	0.4						
	V10Gy			27.3	0.6	6.3	12.4	74.2	3.9	26.3	1.1	31.8	**3.9****	**3.4****

(*continued on next page*)

Table 1 (*Continued*)

Structure	*Metric*	*RTOG 0915*	*VMAT*		*IMPT*		*TB 3b*		*TB 5b*		*TB 10b*		*TB 5b-VMAT*	*TB 5b-IMPT*
			1-6	*7*	*1-6*	*7*	*1-6*	*7*	*1-6*	*7*	*1-6*	*7*	*1-6*	*1-6*
Lung (c)	mean		0.4	1.1				0.1	0.1	0.4	0.1	1.0	**-0.3****	0.1
	V20Gy													
	V10Gy			0.2			2.4	5.8	3.3		1.2	0.1	3.3	3.3
	V5Gy		0.5	23.8			5.1	9.7	16.9	67.0	22.1	112.0	16.4	16.9
Lung (i)	mean		2.6	5.1	1.7	3.8	2.0	4.3	1.4	4.3	1.9	4.3	-1.1	-0.2
	V20Gy		40.5	197.9	43.5	150.6	42.7	183.7	38.8	184.2	37.0	173.5	-1.7	-4.6
	V10Gy		147.4	347.4	112.9	255.7	179.4	329.7	142.1	314.6	135.0	312.5	-5.3	29.3
	V5Gy		323.1	439.2	197.6	331.4	253.8	373.2	270.5	389.8	258.1	377.7	-52.6	**72.9****
Lungs-ITV†	mean		1.4	3.0	0.8	1.8	1.0	2.2	1.0	2.3	1.0	2.5	**-0.5****	0.2
	V20Gy		37.2	178.3	40.2	131.0	39.5	164.1	35.7	164.5	33.9	153.9	-1.5	-4.5
	V10Gy		144.0	328.0	109.7	236.0	178.8	315.8	142.3	294.9	132.9	293.0	-1.8	**32.6****
	V7.4Gy	<1000cm^3	210.1	373.0	147.1	275.4	220.4	340.4	213.8	354.8	202.1	354.8	3.7	**66.7****
	V7Gy	<1500cm^3	223.7	381.0	153.9	281.7	226.1	344.4	224.9	371.6	214.8	370.8	1.2	**71.0****
	V5Gy		320.3	443.5	194.2	311.7	255.5	363.2	283.9	437.1	276.9	470.0	-36.5	**89.6****
body	mean		0.6	1.7	0.2	0.8	0.4	1.3	0.4	1.4	0.4	1.4	**-0.2****	**0.1****

* 0.01 < p-value < 0.05;

** p-value < 0.01; paired t-test with alpha = 0.05

† Note: RTOG0915 requirements are for Lungs-GTV

Table 2 FLASH-percentages using different dose-rate calculation methods (UHDR-contribution [UHDRc], dose-averaged dose-rate [DADR], PBS dose-rate and average dose-rate [ADR]) for multiple FLASH dose (D)- and dose-rate (DR)-thresholds, minimum spot times (minST), maximum nozzle currents (maxN) and gantry current techniques (energy-layer based [EB] and spot-based [SB]). Values give mean (std) for patient 1-6 and the values for patient 7.

DR-threshold (Gy/s)		*40*				*100*			
D-threshold (Gy)		*4*				*8*			
minST (ms)		*0.5*		*2*		*0.5*		*2*	
maxN (nA)		*400*		*200*		*400*		*200*	
GC		*EB*	*SB*	*EB*	*SB*	*EB*	*SB*	*EB*	*SB*
UHDRc	1-6	78.6 (1.5)	80.0 (1.7)	69.0 (1.5)	77.8 (1.5)	33.8 (6.8)	39.3 (5.4)	9.6 (7.9)	31.3 (6.8)
	7	84.0	86.3	69.5	81.7	33.5	40.4	4.9	27.4
DADR	1-6	81.3 (1.9)	81.3 (1.9)	81.3 (1.9)	81.2 (1.9)	43.6 (4.7)	43.6 (4.7)	40.1 (6.1)	43.6 (4.7)
	7	88.3	88.3	88.3	88.3	46.5	46.5	41.1	46.5
PBS	1-6	81.2 (1.8)	81.3 (1.9)	26.8 (23.1)	81.1 (1.8)	35.3 (10.9)	43.6 (4.7)	0.0 (0.0)	27.4 (13.4)
	7	72.6	87.6	0.6	40.9	3.2	24.6	0.0	1.3
ADR	1-6	79.2 (2.2)	81.2 (1.9)	8.3 (13.1)	76.1 (3.8)	20.4 (21.1)	43.2 (4.5)	1.0 (0.0)	10.9 (15.5)
	7	0.6	34.4	0.0	0.0	0.0	0.0	0.0	0.0

(maxN) are currently feasible (0.5 ms/400 nA) or clinically used (2 ms/200 nA). In all scenarios the DADR results in the highest percentage of FLASH-dose, followed by the UHDRc, PBS-DR, and ADR. Because the first 2 methods do not include scanning time, it was expected that their dose-rates would end up higher than for the PBS-DR and ADR methods. This is confirmed by Fig. 1, which shows for clinically used parameters (EB GC, minST = 2 ms, maxN = 200 nA) the dose (A) and dose-rate for all 4 calculation methods (B-F) in a single beam of a 5-beam TB-plan. Here the DADR reaches dose-rates over 250 Gy/s, while the PBS-DR and ADR only achieve ~70 Gy/s and ~50 Gy/s, which are barely higher than the lower threshold of 40 Gy/s and do not meet the threshold of 100 Gy/s. For the larger tumor the dose-rates are even lower: DADR achieves around 200 Gy/s, and PBS-DR and ADR only go up to ~50 Gy/s and ~10 Gy/s (Fig. E3).

Because the UHDRc and DADR easily exceed the dose-rate threshold T_{DR}, the FLASH-percentages of these dose-rates depend mainly on the dose threshold T_D. The PBS-DR and ADR percentages are more dependent on T_{DR} for less favorable machine settings (EB GC, high minST, low maxN), but this shifts to T_D-dependence as advantageous machine settings increase the dose-rates. As expected, the highest FLASH-percentage (~80%) is found for FLASH-requirements of 40 Gy/s and 4 Gy, with a SB GC, maxN = 400 nA and minST = 0.5 ms. This percentage is similar for all dose-rate methods and approaches the percentage of dose exceeding T_D, implying that for these parameters all calculation methods achieve sufficiently high dose-rates. For T_D = 8 Gy and T_{DR} = 100 Gy/s FLASH-percentages are much lower and vary between 0% to 46%.

From Table 2 it also follows that a SB GC leads to higher FLASH-percentages compared with an EB GC. This difference is more pronounced for 2 ms/200 nA settings than for 0.5 ms/400 nA because there exists a certain MU threshold which is proportional to the multiplication of the minimum spot time and maximum nozzle current. Only spots with less MUs than this threshold are influenced by changing the GC technique (by using a higher current for the SB GC than for the EB GC). Spots with more MUs than this threshold are delivered at the highest current feasible by the machine, both for an EB GC and a SB GC. Therefore, using a SB GC instead of an EB GC is more beneficial in plans with many low MU spots or when the MU threshold is high (achieved by increasing the minimum spot time and maximum nozzle current).

Figure 2 shows how the FLASH-percentages are influenced by the choice of T_D and T_{DR}. The upper figures show that dose-rate threshold T_{DR} barely affects the FLASH-percentages of the UHDRc and DADR methods, and PBS-DR and ADR percentages decrease strongly for higher T_{DR} (for a constant T_D). Dose threshold T_D does strongly influence the percentages of UHDRc and DADR (for a constant T_{DR}), as demonstrated by the lower figures.

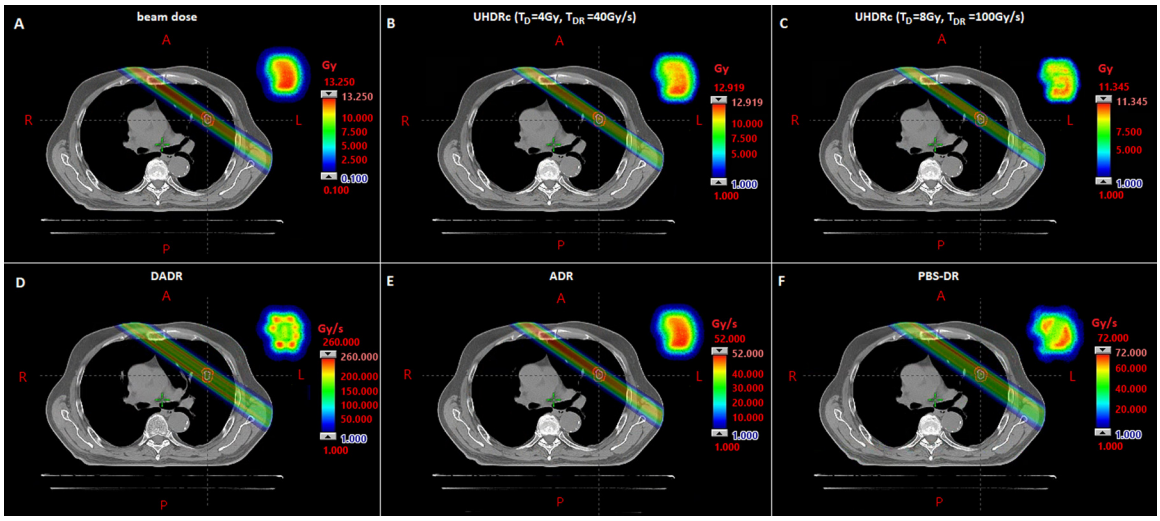

Fig. 1 Dose A, ultra-high dose-rate radiotherapy contribution (UHDRc) with FLASH-threshold of 4 Gy/40 Gy/s B and 8 Gy/100 Gy/s C, and different dose-rates (D, dose-averaged dose-rate [DADR]; E, average dose-rate [ADR]; and F, proton pencil-beam scanning dose-rate with a dose cut-off of 0.01 Gy) of a single beam of a 5-beam transmission beam-plan (for a small lesion). In the right-upper corner the corresponding cross-section of the beam is given. Delivery parameters are minST = 2ms, maxN = 200nA, energy-layer based gantry current (EBGC).

FLASH-modified dose

Table 3 gives ribs and lungs-ITV dose statistics of the IMPT-plans, 5-beam TB-plans and the 3 FMD scenarios (calculated using UHDRc and ADR, as these methods result in high and low FLASH-percentages; and FLASH-factor = 1.4). The DVHs of these plans for a single patient are shown in Figure 3. The Supplementary Materials

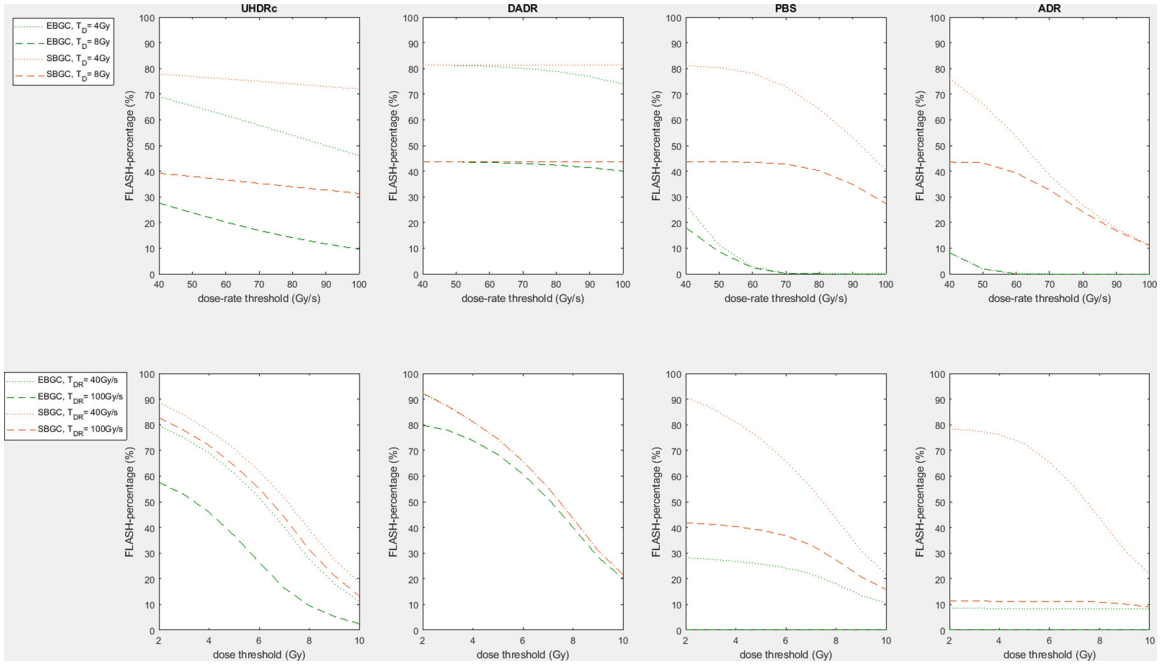

Fig. 2 The upper figures show the influence of dose-rate threshold T_{DR} on the FLASH-percentage for energy-layer based or spot-based gantry-current and T_D = 4 Gy/8 Gy using different dose-rate calculation methods (ultra-high dose-rate radiotherapy contribution [UHDRc], dose-averaged dose-rate [DADR], proton pencil-beam scanning dose-rate, and average dose-rate [ADR]). The lower figures show for the same dose-rate calculation methods the influence of dose threshold T_D on the FLASH-percentage for energy-layer based or spot-based gantry-current and T_{DR} = 40 Gy/s/100 Gy/s. The percentages are averages of all 6 small lesion patients. Delivery parameters are minST = 2ms, maxN = 200nA.

Table 3 ribs and lungs-ITV dose statistics of intensity-modulated proton therapy (IMPT), 5-beam transmission beam (TB) plans and three FLASH-modified dose (FMD) scenarios using UHDR-contribution (UHDRc) and average dose-rate (ADR). The FMD scenarios are (1) currently used parameters of minST=2ms, maxN=200nA and EB GC for FLASH requirements of 4Gy and 40Gy/s, (2) optimal parameters of minST=0.5ms, maxN=400nA and SB GC for FLASH-requirements of 4Gy and 40Gy/s and for (3) 8Gy and 100Gy/s. The FLASH-factor is 1.4.

Structure	*Metric*	*IMPT*		*TB 5b*		*UHDRc4Gy, 40Gy/s2ms, 200nA, EB*		*UHDRc4Gy, 40Gy/s0.5ms, 400nA, SB*		*UHDRc8Gy, 100Gy/s0.5ms, 400nA, SB*		*ADR4Gy, 40Gy/s2ms, 200nA, EB*		*ADR4Gy, 40Gy/s0.5ms, 400nA, SB*		*ADR8Gy, 100Gy/s0.5ms, 400nA, SB*	
		1-6	*7*	*1-6*	*7*	*1-6*	*7*	*1-6*	*7*	*1-6*	*7*	*1-6*	*7*	*1-6*	*7*	*1-6*	*7*
Ribs	mean	0.7	2.9	1.6	5.1	1.3	4.1	1.0	3.8	1.3	4.5	1.5	5.1	1.0	4.6	1.3	5.1
	max	21.9	36.5	23.0	38.4	17.7	30.1	14.4	28.0	20.5	34.3	22.5	38.4	14.3	35.9	20.3	38.3
	V22Gy	1.1	42.9	1.3	54.7	0.4	26.9	0.0	20.1	0.5	34.6	1.3	54.7	0.0	37.2	0.4	54.7
	V16Gy	3.1	71.8	5.6	89.7	1.9	61.6	0.7	57.1	2.4	71.1	5.5	89.7	0.7	76.3	2.3	89.7
	V12Gy	9.2	97.0	19.3	121.8	6.7	94.8	2.4	89.6	8.5	107.7	15.7	121.8	2.3	110.6	8.0	121.8
Lungs-ITV	mean	0.8	1.8	1.0	2.3	0.8	1.8	0.6	1.7	0.8	2.0	1.0	2.3	0.6	2.0	0.8	2.3
	V20Gy	40.2	131.0	36.0	160.4	20.3	98.3	9.6	89.4	23.4	120.1	33.6	160.4	9.2	124.8	22.5	160.4
	V10Gy	110.2	236.0	142.3	281.3	90.2	242.7	57.2	234.7	95.0	257.2	130.5	281.3	56.3	260.7	92.8	281.3
	V7Gy	154.6	281.7	224.7	354.2	168.3	301.4	116.3	295.9	173.7	344.8	224.7	354.2	114.7	350.3	166.4	354.2
	V5Gy	195.0	311.7	282.0	417.1	244.6	379.3	191.0	364.2	273.1	417.1	282.0	417.1	189.2	417.1	266.1	417.1

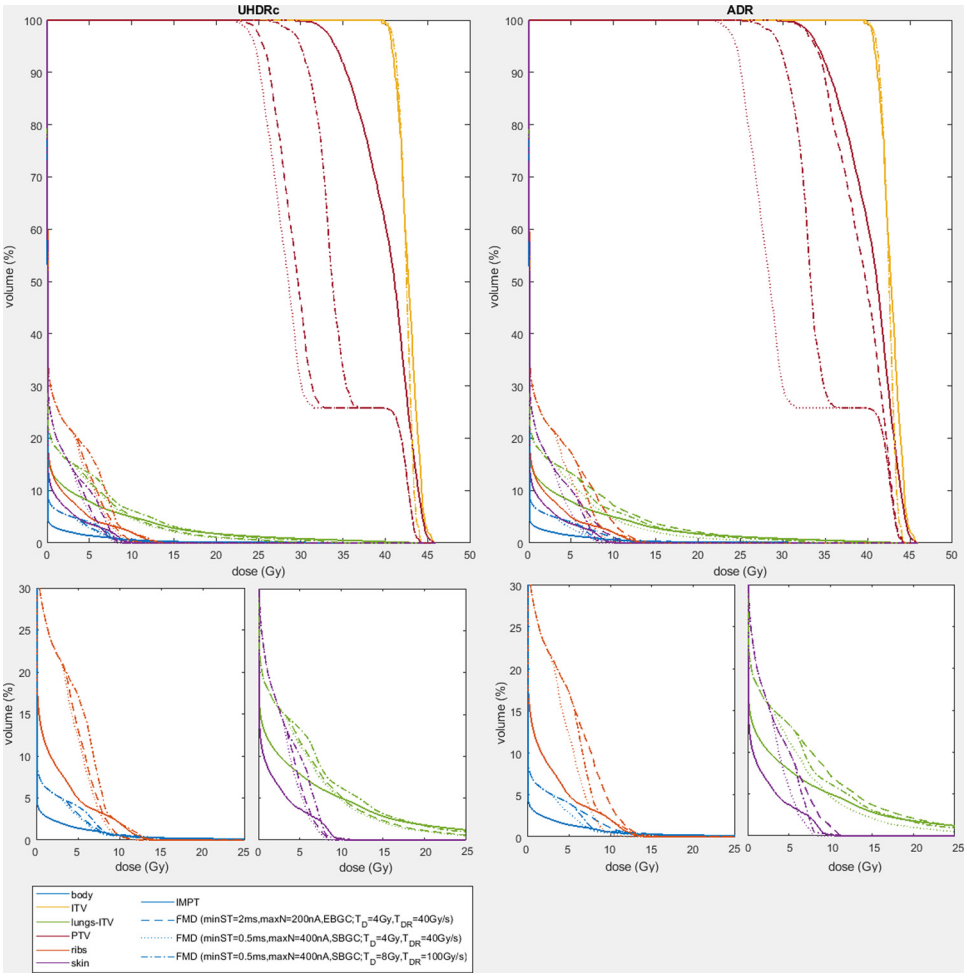

Fig. 3 Dose-volume histograms of intensity modulated proton therapy-plan and 3 FLASH-modified doses (using ultra-high dose-rate radiotherapy contribution [UHDRc] and average dose-rate [ADR]): (1) minST = 2 ms, maxN = 200 nA, energy-layer based (EB) GC; T_D = 4 Gy, T_{DR} = 40 Gy/s, (2) minST = 0.5 ms, maxN = 400 nA, spot-based (SB) gantry-current (GC); T_D = 4 Gy, T_{DR} = 40 Gy/s and (3) minST = 0.5 ms, maxN = 400 nA, SB GC; T_D = 8 Gy, T_{DR} = 100 Gy/s, for a single patient. FLASH-factor = 1.4. Note that the kink in the dose volume histograms of the planning target volume originates from the fact that the dose of the internal planning volume is not modified.

(Table E1 and E2 and Fig. E4) include the dose statistics and DVHs of the other patients and other dose-rate calculation methods and for FLASH-factor = 1.8.

The FMDs obtained using UHDRc are better than for ADR, which is expected based on the higher FLASH-percentages. However, for the optimal scenario (FLASH-requirements: 4 Gy and 40 Gy/s, machine parameters: minST = 0.5 ms, maxN = 400 nA and SB GC) even the ADR-FMD approaches IMPT (for the ribs, body, and skin around 7-8 Gy and lungs-ITV around 10 Gy). For the larger tumor, the 3 UHDRc-FMDs are comparable and also reach IMPT DVH (body and skin around 8 Gy and ribs and lungs-ITV around 12 Gy), but the ADR-FMDs do not, because the larger fields require more scanning time.

Irradiation times

For minST = 2 ms and maxN = 200 nA the total beam irradiation times (including scanning time) were for the small lesions on average 0.31 s for EB GC and 0.11 s for SB GC, leading to total irradiation times of 1.57 s for EB GC and 0.56 s for SB GC. The larger tumor had an average beam irradiation time of 1.18 s/0.49 s and a total irradiation time of 5.89 s/2.45 s for EB/SB GC. For the most advantageous beam parameters minST = 0.5 ms and maxN = 400 nA, the beam irradiation times for the small lesions reduced to on average 0.09 s/0.06 s for EB/SB GC with a total irradiation time of 0.47 s/0.28 s for EB/SB GC. The average beam time of the larger tumor was 0.36 s/0.22 s, resulting in a total irradiation time of

1.81 s/1.09 s, for EB/SB GC. Specific beam and patient data can be found in the Table E3.

Discussion

In this article we focused on evaluating the possible FLASH-contribution for single fraction, high dose radiation therapy, using a model of a single fraction of 34 Gy for small lung lesions. We found that 5-beam TB-plans can achieve similar or lower OAR doses to VMAT, but have higher rib, skin, and ipsilateral lung dose compared with Bragg-peak IMPT, due to TB exit dose. It is important to realize that the IMPT-plans used in this article have been robustly optimized, based on the CT scan, but do not take density differences between CT scan and treatment, nor changes during treatment, into account. The IMPT-plans will therefore not be as good in reality, but they have been included because they likely represent the best possible plans.

We have mainly focused on smaller lesions because currently at our facility a single fraction of 34 Gy is mostly used for relatively small tumors, which is consistent with the literature.[47,48] However, the RTOG 0915 allows for single fraction delivery to larger tumors as well and therefore we have included one larger lesion as well. This lesion was added mainly for illustrative purposes, showing that the DR calculation methods are significantly influenced by tumor size. The difference was particularly large for the PBS-DR and ADR, which not only consider the local doses and dose-rates, but are also dependent on scanning time or a spot dose threshold, and if one of these methods turns out to be of biological relevance, it will prove difficult to achieve a FLASH-effect for larger tumors.

As it is not known yet which dose-rate calculation is most representative of the FLASH-effect, we examined several methods and analyzed the amount of FLASH-dose for different FLASH dose and dose-rate thresholds and machine parameters. We found that (1) dose-rate methods based on spot dose-rates (excluding scanning time) easily exceed FLASH dose-rates mentioned in literature (up to 100 Gy/s[3,26]), making T_D the limiting factor for FLASH; (2) methods including scanning time have difficulty achieving sufficiently high dose-rates, but this can be improved by adjusting machine parameters (eg, increasing maxN or decreasing minST); (3) with favorable machine parameters there is not much difference in FLASH-percentage between dose-rate methods, implying that the dose threshold T_D is the limiting factor; (4) SB GC leads to higher dose-rates compared with EB GC and this difference is more pronounced in plans with many low MU spots and for higher minST and lower maxN; and (5) it is possible to increase the FLASH-percentage by using a SB GC instead of an EB GC or by trying to achieve a lower minST (with corresponding higher maxN) and that the preference for one of these options depends on the FLASH-thresholds: for lower T_D and T_{DR} it is not that useful to use a SB GC instead of a EB GC, but decreasing the minST can have a large effect, and for higher T_D and T_{DR} the percentages increase a lot for a SB GC. Another important observation is that for T_D = 8 Gy/ T_{DR} = 100 Gy/s the FLASH-percentage is only between 0% to 46%, meaning that even for single-fraction 34 Gy almost no FLASH is present and finding a clinical application for FLASH may prove problematic.

Some of our findings were confirmed by earlier research, such as the DADR reaching higher values than the PBS-DR.[34] However, that publication observed that the PBS-DR is highest at the beam edges and that the DADR was more evenly distributed, while we found that neither of these methods have a uniform distribution (Fig. 1). These differences might be explained by the fact that we focus on smaller lesions and show that beam characteristics influence the dose-rate distribution significantly.

For the small lesions, the UHDRc-FMDs approached the IMPT DVH, as did the optimal ADR-FMD (for doses >8 Gy for ribs, skin and body and for doses >10 Gy for the lungs-ITV). The other 2 scenarios (low FLASH-thresholds with clinical machine parameters and high FLASH-threshold with improved machine parameters) are comparable to each other for both UHDRc and ADR, suggesting that machine parameters might be able to compensate for unadvantageous FLASH-requirements.

Furthermore, the higher standard deviation for the PBS-DR and ADR methods suggests there is more variation in FLASH-percentages between patients, meaning that these methods are more sensitive to plan characteristics. This is likely caused by the inclusion of scanning time, which is highly dependent on spot locations, and is longer for larger tumors. The standard deviation generally increases for unfavorable FLASH-requirements for all calculation methods, which means that the corresponding doses and dose-rates are likely to be close to T_D and T_{DR} and result in either no FLASH or a large amount of FLASH.

The PBS-DR also depends on the dose-threshold $T_{D,PBS}$ of 1 cGy. This threshold determines which spots are included in the calculation and can therefore influence the DR significantly, especially for larger fields. It might make more sense to use a method that considers the time necessary to deliver a certain minimum dose, which has been described earlier.[49]

We concentrated on single fraction 34 Gy lung SBRT because beam doses >4 to 10 Gy are frequently considered necessary for the FLASH-effect, which if correct, means that this will be difficult, if not impossible, to achieve for most fractionated schemes. Because single-fraction 34 Gy for ES-NSCLC was demonstrated to be just as effective as multifraction schemes[20] and can have other benefits, such as patient ease and lower costs, it

merits consideration as a candidate for moving FLASH into the clinic. Other advantages are a small number of OARs and the possibility to monitor radiation-induced damage by evaluating lung fibrosis on CT-scans. Lung fibrosis presents a practical problem for follow-up, as it can make recurrent tumors harder to detect.[21,22] If a FLASH-effect reduces the amount of fibrosis, it will be of clinical significance both by reducing potential toxicity, as well as improving recurrence detection. Specifically patients with multiple lung metastases, who are treated more often with lung SBRT after the trial for Comprehensive Treatment of Oligometastases (COMET-trial), can benefit from a FLASH-effect. The first COMET-trial demonstrated how patients with oligometastases (≤5 metastases) showed improved progression-free survival and overall survival after SBRT treatment[23-25] and a second trial (SABR-COMET-10) will investigate the effect of SBRT in patients with 4 to 10 metastates.[50] Treatment of a single lesion may not result in too high lung doses, but the risk of radiation pneumonitis and fibrosis increases when multiple lesions are treated, and a FLASH-effect can be of clinical significance.

Another clinical benefit is that the short irradiation time of TB-FLASH (<1.5 s) makes it easier to treat during short breath-holds. The tumor position could be monitored using fluoroscopy,[51,52] irradiating only when the tumor is in the right position.

The lungs are also a good site for the use of TBs, due to their low tissue density. TBs are not influenced by density changes and range uncertainty. Additionally, they do not require layer switching, facilitate dose verification by distally placed detectors and can be delivered much faster (~0.3 s for smaller lesions [ITV <9 cm^3] and <1.5 s for a larger tumor [ITV = 55 cm^3]), making it possible to deliver the entire fraction withing a single breathing phase, thereby avoiding troublesome breath-hold techniques. The effects of UHDRs on the linear energy transfer at and around the Bragg-peak can also be ignored. However, the main disadvantage of TBs is the lack of use of the Bragg-peak and in particular the low dose deposition behind it. Currently, hedgehog filters are believed to be the solution to this problem, but these also have their drawbacks: they are highly prone to errors, make planning more difficult, are patient- and beam-specific, and need to be made in such a precise manner that, in contrast to TBs, it is currently not easily possible to use them clinically. However, it has been demonstrated recently that FLASH dose-rates using single-energy Bragg-peaks are achievable using range shifters and inverse optimization.[53]

Very high energy electron radiation therapy, achieving energies up to 250 Mev, can also be an interesting possibility for FLASH-RT, as similar dosimetry to that of TBs has been simulated and measured.[54,55] Because it is still uncertain what exactly leads to the FLASH-effect, multiple assumptions have had to be made in this analysis. The exact dose-rate and dose threshold are still unknown,[7,9] and we therefore decided to use multiple thresholds (40/100 Gy/s and 4/8 Gy). However, it is likely there is a gradually increasing effect based on dose-rate (and dose), rather than a definite cut-off threshold. In addition, there are several ways to calculate dose-rate, and it is not known which one is applicable to calculate the FLASH-effect. Therefore we showed the results for a variation of dose-rate calculations. Also, the values for minST and maxN have been selected based on clinically used parameters and literature,[38,39] but other values are possible and may give rise to other conclusions. Furthermore, we have considered each beam separately, based on the oxygenation hypothesis and the fact it only takes ~ 10^{-3}s to 10^{-2}s to reoxygenate the tissue[44] (compared with >30 s between beam irradiations), leading to a return to the initial state before a subsequent irradiation. However, this is just an assumption based on the available literature, but more radiobiologic research would be needed.

Additional research is not only required to understand the mechanism behind the FLASH-effect, but also to clarify other radiobiological aspects. For instance, (1) the (amount of) FLASH-effect might be tissue specific; (2) the influence of time between spots/beams/fractions on the FLASH-effect is unknown; as is (3) the radiobiologically relevant definition of dose-rate; and (4) factors such as dose and tissue oxygen levels may also play some part in the origination of the FLASH-effect.[45] It would also be useful to investigate how to increase the dose-rate by adjusting machine parameters and plan characteristics, such as minimizing spot times, increasing the gantry current or increasing spot MUs by using spot reduction methods.[36] Changing the scanning pattern can also influence the FLASH-percentage, in particular if a dose-rate calculation method including scanning time, such as ADR and PBS-DR, turns out to be important for the FLASH-effect. Lastly, we focused on transmission beams as UHDR proton treatments are now possible using TBs, unlike Bragg-peak IMPT. But it is expected that also Bragg-peak UHDR treatments will become possible in the coming years.

Conclusions

In this article we have focused on single-fraction 34 Gy lung SBRT and showed how 5-beam TB-plans can achieve similar plan quality to VMAT, but have higher rib, skin and ipsilateral lung dose compared with IMPT. We have also analyzed the amount of FLASH-dose for multiple dose-rate calculation methods, FLASH-thresholds and delivery parameters and found that dose-rate calculation methods excluding scanning time (UHDRc and DADR) easily achieve FLASH dose-rates, while the PBS-DR and ADR struggle to meet the dose-rate requirements. However, by adjusting machine parameters (decreasing minST/increasing maxN or using a SB GC instead of an EB GC) high enough dose-rates can be achieved for all

calculation methods, meaning that in the end the FLASH dose threshold T_D is the limiting factor for FLASH.

Acknowledgments

We thank Jessica Perez, Michael Folkerts, and Eric Abel for their contribution to discussion about the research.

Supplementary materials

Supplementary material associated with this article can be found in the online version at doi:10.1016/j.adro.2022.100954.

References

1. Favaudon V, Caplier L, Monceau V, et al. Ultrahigh dose-rate FLASH irradiation increases the differential response between normal and tumor tissue in mice. *Sci Transl Med*. 2014;6:245.
2. Montay-Gruel P, Petersson K, Jaccard M, et al. Irradiation in a flash: Unique sparing of memory in mice after whole brain irradiation with dose-rates above 100 Gy/s. *Radiother Oncol*. 2017;124:365–369.
3. Vozenin MC, De Fornel P, Petersson K, et al. The advantage of FLASH radiotherapy confirmed in mini-pig and cat-cancer patients. *Clin Cancer Res*. 2019;25:35–42.
4. Bourhis J, Sozzi WJ, Jorge PG, et al. Treatment of a first patient with FLASH-radiotherapy. *Radiother Oncol*. 2019;139:18–22.
5. Montay-Gruel P, Acharya MM, Jorge PG, et al. Hypofractionated FLASH-RT as an effective treatment against glioblastoma that reduces neurocognitive side effects in mice. *Clin Cancer Res*. 2021;27:775–784.
6. Ruan J-L, Lee C, Wouters S, et al. Irradiation at ultra-high (FLASH) dose rates reduces acute normal tissue toxicity in the mouse gastrointestinal system. *Int J Radiat Oncol Biol Phys*. 2021;111:1250–1261.
7. Wilson JD, Hammond EM, Higgins GS, Petersson K. Ultra-high dose rate (FLASH) radiotherapy: Silver bullet or fool's gold? *Front Oncol*. 2020;9:1563.
8. Hughes JR, Parsons JL. FLASH radiotherapy: Current knowledge and future insights using proton-beam therapy. *Int J Mol Sci*. 2020;21:6492.
9. Vozenin MC, Hendry JH, Limoli CL. Biological benefits of ultra-high dose rate FLASH radiotherapy: Sleeping beauty awoken. *Clin Oncol*. 2019;31:407–415.
10. Benedict SH, Yenice KM, Followill D, et al. Stereotactic body radiation therapy: The report of AAPM Task Group 101. *Med Phys*. 2010;37:4078–4101.
11. Guckenberger M, Andratschke N, Dieckmann K, et al. ESTRO ACROP consensus guideline on implementation and practice of stereotactic body radiotherapy for peripherally located early stage non-small cell lung cancer. *Radiother Oncol*. 2017;124:11–17.
12. Postmus PE, Kerr KM, Oudkerk M, et al. Early and locally advanced non-small-cell lung cancer (NSCLC): ESMO clinical practice guidelines for diagnosis, treatment and follow-up. *Ann Oncol*. 2017;28:iv1–iv21.
13. Stephans KL, Woody NM, Reddy CA, et al. Tumor control and toxicity for common stereotactic body radiation therapy dose-fractionation regimens in stage I non-small cell lung cancer. *Int J Radiat Oncol Biol Phys*. 2018;100:462–469.
14. Wrona A, Mornex F. Effect of tumor location and dosimetric predictors for chest wall toxicity in single-fraction stereotactic body radiation therapy for stage I non-small cell lung cancer. *Semin Radiat Oncol*. 2021;31:97–104.
15. Whyte RI, Crownover R, Murphy MJ, et al. Stereotactic radiosurgery for lung tumors: Preliminary report of phase I trial. *Ann Thorac Surg*. 2003;75:1097–1101.
16. Le Q-T, Loo BW, Ho A, et al. Results of a phase I dose-escalation study using single-fraction stereotactic radiotherapy for lung tumors. *J Thorac Oncol*. 2006;1:802–809.
17. Fritz P, Kraus H-J, Mühlnickel W, et al. Stereotactic, single-dose irradiation of stage I non-small cell lung cancer and lung metastases. *Radiat Oncol*. 2006;1:30.
18. Singh AK, Gomez-Suescun JA, Stephans KL, et al. One versus three fractions of stereotactic body radiation therapy for peripheral stage I to II non-small cell lung cancer: A randomized, multi-institution, phase 2 trial. *Int J Radiat Oncol Biol Phys*. 2019;105:752–759.
19. Videtic GMM, Hu C, Singh AK, et al. NRG oncology RTCOG 0915 (NCCTG N0927): A randomized phase II study comparing 2 stereotactic body radiation therapy (SBRT) schedules for medically inoperable patients with stage I peripheral non-small cell lung cancer. *Int J Radiat Oncol Biol Phys*. 2015;93:757–764.
20. Videtic GM, Paulus R, Singh AK, et al. Long term follow-up on NRG Oncology RTOG 0915 (NCCTG N0927): A randomized phase II study comparing 2 stereotactic body radiation therapy schedules for medically inoperable patients with stage I peripheral non-small cell lung cancer. *Int J Radiat Oncol Biol Phys*. 2019;103:1077–1084.
21. Dahele M, Palma D, Lagerwaard F, Slotman B, Senan S. Radiological changes after stereotactic radiotherapy for stage I lung cancer. *J Thorac Oncol*. 2011;6:1221–1228.
22. Dahele M, van Sörnsen de Koste JR, van de Ven PM, Spoelstra F, Slotman BJ, Senan S. Parenchymal lung changes on computed tomography after stereotactic radiotherapy using high dose rate flattening filter free beams. *Radiother Oncol*. 2015;114:357–360.
23. Palma D, Olson R, Harrow S, et al. Stereotactic ablative radiotherapy versus standard of care palliative treatment in patients with oligometastatic cancers (SABR-COMET): A randomized, phase 2, open-label trial. *Lancet*. 2019;393:2051–2058.
24. Olson R, Senan S, Harrow S, et al. Quality of life outcomes after stereotactic ablative radiation therapy (SABR) versus standard of care treatments in the oligometastatic setting: A secondary analysis of the SABR-COMET randomized trial. *Int J Radiation Oncol Biol Phys*. 2019;105:943–947.
25. Palma D, Olson R, Harrow S, et al. Stereotactic ablative radiotherapy for the comprehensive treatment of oligometastatic cancers: Long-term results of the SABR-COMET phase II randomized trial. *J Clin Oncol*. 2020;38:2830–2838.
26. Montay-Gruel P, Bouchet A, Jaccard M, et al. X-rays can trigger the FLASH effect: Ultra-high dose-rate synchrotron light source prevents normal brain injury after whole brain irradiation in mice. *Radiother Oncol*. 2018;129:582–588.
27. Diffenderfer ES, Verginadis II, Kim MM, et al. Design, implementation, and in vivo validation of a novel proton FLASH radiation therapy system. *Int J Radiat Oncol Biol Phys*. 2020;106:440–448.
28. Darafsheh A, Hao Y, Zwart T, et al. Feasibility of proton FLASH irradiation using a synchrocyclotron for preclinical studies. *Med Phys*. 2020;47:4348–4355.
29. van Marlen P, Dahele M, Folkerts M, Abel E, Slotman BJ, Verbakel WFAR. Bringing FLASH to the clinic: Treatment planning considerations for ultrahigh dose-rate proton beams. *Int J Radiat Oncol Biol Phys*. 2020;106:621–629.
30. Perez J, Magliari A, Folkerts M, et al. FLASH radiotherapy: A look at ultra-high dose rate research and treatment plans. *Abstract PTCOG*. 2019.

31. Mou B, Beltran CJ, Park SS, Olivier KR, Furutani KM. Feasibility of proton transmission-beam stereotactic ablative radiotherapy versus photon stereotactic ablative radiotherapy for lung tumors: A dosimetric and feasibility study. *PLoS One*. 2014;9:e98621.
32. van Marlen P, Dahele M, Folkerts M, Abel E, Slotman BJ, Verbakel WFAR. Ultra-high dose rate transmission beam proton therapy for conventionally fractionated head and neck cancer: Treatment planning and dose-rate distributions. *Cancers*. 2021;13:1859.
33. FAST-01 FLASH therapy trial. Available at: https://clinicaltrials.gov/ct2/show/NCT04592887. Accessed May 2, 2022.
34. Kang M, Wei S, Choi JI, Simone II CB, Lin H. Qualitative assessment of 3D dose rate for proton pencil beam scanning FLASH radiotherapy and its application for lung hypofractionation treatment planning. *Cancers*. 2021;13:3549.
35. Folkerts M, Abel E, Busold S, Perez JR, Krishnamurthi V, Ling CC. A framework for defining FLASH dose rate for pencil beam scanning. *Med Phys*. 2020;47:6396–6404.
36. van de Water S, Safai S, Schippers JM, Weber DC, Lomax AJ. Towards FLASH proton therapy: The impact of treatment planning and machine characteristics on achievable dose rates. *Acta Oncol*. 2019;58:1463–1469.
37. Safai S, Bula C, Meer D, Pedroni E. Improving the precision and performance of proton pencil beam scanning. *Translat Cancer Res*. 2012;1:196–206.
38. Bula C, Belosi MF, Eichin M, Hrbacek J, Meer D. Dynamic beam current control for improved dose accuracy in PBS proton therapy. *Phys Med Biol*. 2019;64: 175003.
39. Pedroni E. Proton beam delivery technique and commissioning issues: Scanned protons. Educational meeting PTCOG 2008.
40. Jin J-Y, Gu A, Wang W, Oleinick NL, Machtay M, Kong F-MS. Ultra-high dose rate effect on circulating immune cells: A potential mechanism for FLASH effect? *Radiother Oncol*. 2020;6(149):55–62.
41. Spitz DR, Buettner GR, Petronek MS, et al. An integrated physicochemical approach for explaining the differential impact of FLASH versus conventional dose rate irradiation on cancer and normal tissue responses. *Radiother Oncol*. 2019;139:23–27.
42. Adrian G, Konradsson E, Lempart M, Bäck S, Ceberg C, Petersson K. The FLASH effect depends on oxygen concentration. *Br J Radiol*. 2019;92: 20190702.
43. Petersson K, Adrian G, Butterworth K, McMahon SJ. A quantitative analysis of the role of oxygen tension in FLASH radiotherapy. *Int J Radiat Oncol Biol Phys*. 2020;107:539–547.
44. Zhou S, Zheng D, Fan Q, et al. Minimum dose rate estimation for pulsed FLASH radiotherapy: A dimensional analysis. *Med Phys*. 2020;47:3243–3249.
45. Rothwell BC, Kirkby NF, Merchant MJ, et al. Determining the parameter space for effective oxygen depletion for FLASH radiation therapy. *Phys Med Biol*. 2021;66: 055020.
46. Chabi S, To THV, LeaVitt R, et al. Ultra-high-dose-rate FLASH and conventional-dose-rate irradiation differentially affect human acute lymphoblastic leukemia and normal hematopoiesis. *Int J Radiat Oncol Biol Phys*. 2021;109:819–829.
47. Nicosia L, Reverberi C, Agolli L, et al. Long term results of single high dose stereotactic body radiotherapy in the treatment of primary lung tumors. *Sci Rep*. 2019;9:15498.
48. Kalinauskaite G, Tinhofer I, Kufeld M, et al. Radiosurgery and fractionated stereotactic body radiotherapy for patients with lung oligometastases. *BMC Cancer*. 2020;20:404.
49. Krieger M, van de Water S, Folkerts MM, et al. A quantitative FLASH effectiveness model to reveal potentials and pitfalls of high dose rate proton therapy. *Med Phys*. 2022;49:2026–2038.
50. Palma D, Olson R, Harrow S, et al. Stereotactic ablative radiotherapy for the comprehensive treatment 4-10 oligometastatic tumors (SABR-COMET-10): Study protocol for a randomized phase III trial. *BMC Cancer*. 2019;19:816.
51. Hazelaar C, Dahele M, Mostafavi H, van der Weide L, Slotman BJ, Verbakel WFAR. Markerless positional verification using template matching and triangulation of kV images acquired during irradiation for lung tumors treated in breath-hold. *Phys Med Biol*. 2018;63: 115005.
52. Remmerts de Vries IF, Dahele M, Mostafavi H, Slotman BJ, Verbakel WFAR. Markerless 3D tumor tracking during single-fraction free-breathing 10MV flattening-filter-free stereotactic lung radiotherapy. *Radiother Oncol*. 2021;164:6–12.
53. Kang M, Wei S, Choi JI, Lin H, Simone II CB. A universal range shifter and range compensator can enable proton pencil beam scanning single-energy Bragg peak FLASH-RT treatment using current commercially available proton systems. *Int J Radiat Oncol Biol Phys*. 2022;113:203–213.
54. Böhlen TT, Germond JF, Traneus E, et al. Characteristics of very high-energy electron beams for the irradiation of deep-seated targets. *Med Phys*. 2021;48:3958–3967.
55. Whitmore L, Mackay RI, van Herk M, Jones JK, Jones RM. Focused VHEE (very high energy electron) beams and dose delivery for radiotherapy applications. *Sci Rep*. 2021;11:14013.